

Dry-Contact Technique for High-Resolution Ultrasonic Imaging

Hironori Tohmyoh and Masumi Saka

Abstract—To accomplish a high-resolution ultrasonic imaging without wetting a sample, the efficiency of the dry-contact ultrasonic transmission is discussed. In this study, a dry-contact interface is formed on a sample by inserting a thin film between water and a sample, and the pressure is working on the interface by evacuating the air between the film and the sample. A model of dry-contact ultrasonic transmission is presented to assess the signal loss accompanied with the transmission. From the determination of the signal loss caused by the transmission using various films, it was found that the higher frequency ultrasound is transmitted effectively into the sample by selecting an optimum film, which can keep the displacement continuity between the film and the sample during ultrasonic transmission. At last, ultrasonic imaging with the sufficient signal-to-noise ratio (SNR) and high lateral resolution was performed on the delamination in a package and the jointing interface of the ball-grid-array package without wetting the packages.

I. INTRODUCTION

MINIATURIZATION with high-density mounting of the integrated circuit (IC) packages [1], [2] demands a sensitive, nondestructive testing technique, which can achieve higher resolution. In point of accomplishing higher resolution, the immersion ultrasonic technique excels over the other techniques such as X-ray [3], [4], laser ultrasonic [5], and microwave techniques [6]. However, because the ultrasonic technique requires the immersion of a sample; the technique is not desirable for IC package inspection.

Some attempts have been made to transmit the ultrasound into a sample without wetting it. One of these techniques makes use of the dry-coupling transducers [7], [8]. These transducers have an elastomer face layer and can be coupled with the sample by applying a pressure. Liaw *et al.* [7] used the transducers to measure the elastic constants of the ceramic-matrix composites. Techniques using air-coupled transducers are available for the transduction of ultrasound in air so far as the frequencies of some megahertz are used [9]–[14]. The popular types include the piezoelectric ceramic element designed to optimize its transduction in air and the capacitance transducer utilizing the electrostatic force. The transducers are

Manuscript received March 22, 2002; accepted November 13, 2002. This work was partly supported by the Ministry of Education, Culture, Sports, Science and Technology of Japan under Grant-in-Aid for Specially Promoted Research (COE)(2) 11CE2003 and Japan Society for the Promotion of Science under Grant-in-Aid for Scientific Research (B)(2) 12450041.

The authors are with the Department of Mechanical Engineering, Tohoku University, Aramaki, Aoba-ku, Sendai 980-8579, Japan (e-mail: tohmyoh@ism.mech.tohoku.ac.jp).

widely used for applications such as the distance measurement [10], thickness measurement [11], nondestructive evaluation (NDE) of aerospace composites [12], tomographic reconstruction [14], and so on. However, the higher frequency ultrasound, which is enough for performing the high-resolution ultrasonic imaging, is not available by these transducers under the existing conditions.

In contrast with the above techniques, a dry-contact ultrasonic technique (DCUT) has been reported [15], [16]. The DCUT enables us to transmit the higher frequency ultrasound into a sample without wetting it by utilizing a dry-contact interface formed on the sample by inserting a thin film between water and the sample. Moreover, DCUT may enhance the ultrasonic reflection from an inspection object, thereby making it advantageous for applications such as inspection of ball-grid-array (BGA) solder joints.

To accomplish a high-resolution imaging by DCUT, the transmission efficiency is discussed in this paper. A model of DCUT is presented, and the signal loss accompanied with the transmission into a plate of acrylic resin is determined by using the model. From the determination of the signal loss in the cases of inserting various films, it was found that the interception of the higher frequency ultrasound is caused at the dry-contact interface. By utilizing the optimum film, which can keep the displacement continuity between the film and the sample during the transmission of higher frequency ultrasound, the dry-contact ultrasonic imaging, which had the sufficient signal-to-noise ratio (SNR) and high lateral resolution as the immersion technique, was performed on the delamination in a package and the jointing interface of the BGA package without wetting the packages.

II. THEORY OF DRY-CONTACT ULTRASONIC TRANSMISSION

The device of DCUT is shown in Fig. 1. The device has a path control layer between the film and the sample, and the layer has the exhaust paths connected to the center hole. The air surrounded with the film, layer, and sample is evacuated by a vacuum pump through the exhaust paths. The film is attached to the sample by working the pressure between the film and the sample. A dry-contact interface is formed between the film and the sample.

To derive the signal loss accompanied with the DCUT, a transmission model is developed. In the dry-contact transmission system shown in Fig. 2, frequency spectrum of the

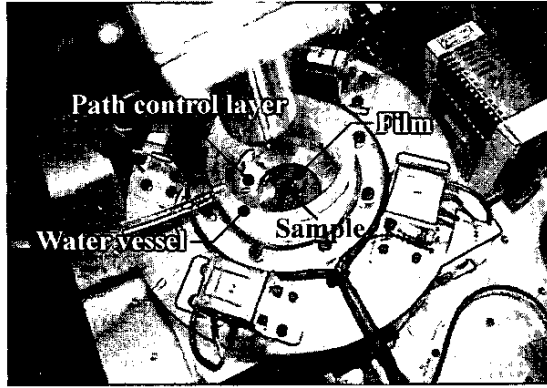


Fig. 1. Details of the dry-contact ultrasonic device.

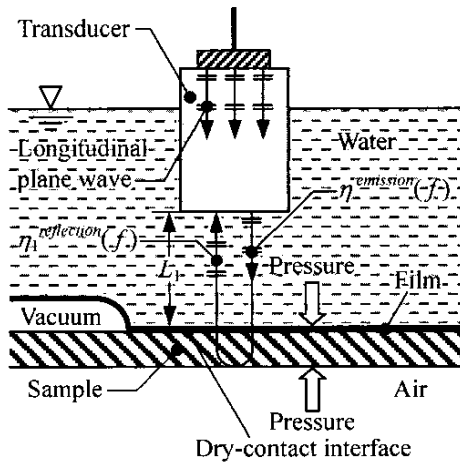


Fig. 2. Schematic of the DCUT.

reflection echo, $\eta_1^{\text{reflection}}(f)$, from the back-wall of a sample may be expressed as:

$$\eta_1^{\text{reflection}}(f) = \eta_1^{\text{emission}}(f) \cdot \alpha_1^{\text{total}}(f) \cdot T_{wfs}(f) \cdot R_{sa} \cdot T_{sfw}(f) \cdot D \cdot C^{PE}(f, p, \beta, \gamma), \quad (1)$$

where f is the frequency; $\eta_1^{\text{emission}}(f)$ is the frequency spectrum of the emission wave from the spherical lens; $\alpha_1^{\text{total}}(f)$ is the total ultrasonic attenuation; $T_{wfs}(f)$ is the transmission coefficient of three media system composed of water, film, and sample; R_{sa} is the reflection coefficient at the back-wall of the sample; D is a term representing the effect of diffraction; and $C^{PE}(f, p, \beta, \gamma)$ is the contact coefficient expressing the signal loss spent at the film/sample interface. The pressure between the film and the sample is denoted by p . The surface roughness of the sample is expressed by two parameters: β describing the height of the roughness and γ describing its distribution. The subscripts w , f , s , and a are for meaning water, film, sample, and air, respectively. The coefficient R_{sa} is given by:

$$R_{sa} = \frac{Z_a - Z_s}{Z_s + Z_a}, \quad (2)$$

where $Z (= \rho \cdot C)$ is the acoustic impedance with the density ρ of a referred medium and the ultrasonic velocity C in the medium. Besides, $\alpha_1^{\text{total}}(f)$ is:

$$\alpha_1^{\text{total}}(f) = \exp\{-[\alpha_s(f) \cdot 2t_s + \alpha_f(f) \cdot 2t_f + \alpha_w(f) \cdot 2L_1]\}, \quad (3)$$

and $T_{wfs}(f)$ is given by [17]:

$$T_{wfs}(f) = \frac{2}{\left(\frac{Z_w}{Z_s} + 1\right) \cos k_f t_f + j \left(\frac{Z_w}{Z_f} + \frac{Z_f}{Z_s}\right) \sin k_f t_f}, \quad (4)$$

where $\alpha(f)$ is the attenuation coefficient of a referred medium; t is the thickness of the medium; L_1 is the water path between spherical lens and film; $k_f (= 2\pi f/C_f)$ is the wavenumber in the film; and $j = \sqrt{-1}$. However, frequency spectrum of the reflection echo in the case of immersion transmission, $\eta_2^{\text{reflection}}(f)$, is given by:

$$\eta_2^{\text{reflection}}(f) = \eta_2^{\text{emission}}(f) \cdot \alpha_2^{\text{total}}(f) \cdot T_{ws} \cdot R_{sw} \cdot T_{sw} \cdot D, \quad (5)$$

where T_{ws} is the transmission coefficient of the system with water and sample. The coefficient T_{ws} and the total ultrasonic attenuation in this case, $\alpha_2^{\text{total}}(f)$, are expressed as:

$$T_{ws} = \frac{2Z_s}{Z_w + Z_s}, \quad (6)$$

and

$$\alpha_2^{\text{total}}(f) = \exp\{-[\alpha_s(f) \cdot 2t_s + \alpha_w(f) \cdot 2L_2]\}, \quad (7)$$

where L_2 is the water path between spherical lens and sample. By dividing (1) by (5), we obtain $C^{PE}(f, p, \beta, \gamma)$ as:

$$C^{PE}(f, p, \beta, \gamma) = \frac{\exp[\alpha_f(f) \cdot 2t_f]}{\exp[\alpha_w(f) \cdot 2(L_2 - L_1)]} \cdot \left| \frac{R_{sw}}{R_{sa}} \right| \cdot \left| \frac{T_{ws} \cdot T_{sw}}{T_{wfs}(f) \cdot T_{sfw}(f)} \right| \cdot N(f), \quad (8)$$

where $N(f) = |\eta_1^{\text{reflection}}(f)/\eta_2^{\text{reflection}}(f)|$. If a perfect interface keeping the displacement continuity between the film and the sample is formed, $C^{PE}(f, p, \beta, \gamma)$ is unity.

III. CHARACTERIZATION OF PLASTIC FILMS

Two kinds of plastic films, polyvinyl chloride (PVC) and polyethylene (PE) films, and a silicone rubber (SIR) sheet were used for dry-contact ultrasonic imaging. The SIR sheet is used as an elastomer face layer of the dry-coupling transducers [7], [8]. The acoustical properties of these films and the sheet are summarized in Table I. The PVC and PE films have t_f of 0.010 and 0.013 mm, and t_f of SIR sheet is 0.200 mm. The impedance Z_f was measured

TABLE I
ACOUSTICAL PROPERTIES OF THE FILMS USED FOR DCUT. FREQUENCY f IS IN MEGAHERTZ.

Film or sheet	Thickness (mm)	Acoustic impedance (MNm ⁻³ s)	Ultrasonic velocity (m/s)	Attenuation coefficient (1/mm)
PVC	0.010	1.833	16.32	$0.0090 f^2 - 0.0063 f$
PE	0.013	1.751	1933	$0.0002 f^2 + 0.1649 f$
SIR	0.200	2.192	1828	$0.0011 f^2 - 0.0470 f$

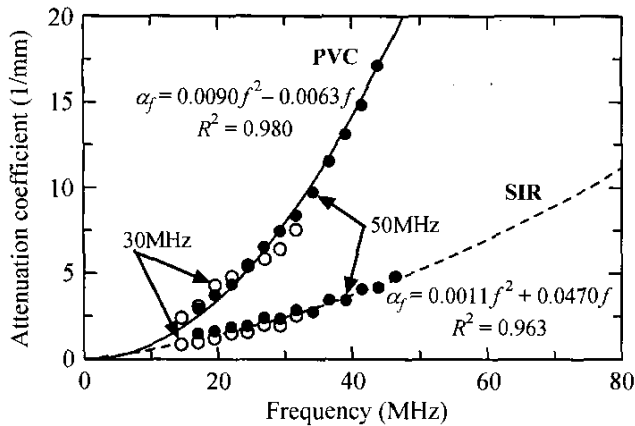


Fig. 3. Ultrasonic attenuation behavior for PVC film and SIR sheet.

by the method described by Kumar *et al.* [18]. Dividing Z_f by the measured density, we determined C_f .

The coefficient $\alpha_f(f)$ was measured by the technique shown in the Appendix. Two transducers with nominal frequencies of 30 and 50 MHz were used. The transducer with 30 MHz nominal frequency has a focal length, z_0 , of 19.05 mm and a diameter of the piezoelectric element, $2a$, of 6.35 mm. The length z_0 of 50 MHz transducer is 12.7 mm and of $2a$ is 6.35 mm. A plate of AISI 304 stainless steel was used as a reflector, and the reflection echoes from the plate's surface were recorded in both cases of with and without film. The impedance Z_w used in (A5) was 1.506 MNm⁻³s. The coefficient $\alpha_f(f)$ of PVC film and SIR sheet obtained by the proposed technique in the relation with f is shown in Fig. 3. The relationship can be approximated by a quadratic form. The coefficient $\alpha_f(f)$ also is summarized in Table I.

IV. EXPERIMENTAL RESULTS

To select the optimum film, which can realize the most effective transmission, the DCUT using PVC and PE films and SIR sheet was performed on the acrylic resin. The SNR, the lateral resolution, d^{PE} , and $C^{PE}(f, p, \beta, \gamma)$ are determined.

A. Dry-Contact Ultrasonic Transmission

The back-wall echoes of a plate of acrylic resin having t_s of 2 mm, β of 0.07 μ m, and γ of 4 μ m were recorded by

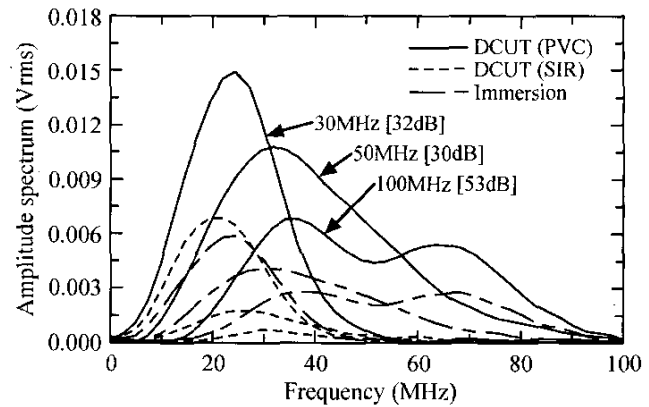


Fig. 4. Amplitude spectra of the back-wall echoes received by the DCUTs using PVC film and SIR sheet and the immersion technique.

DCUTs using PVC and PE films and SIR sheet in the air. The arithmetical mean deviation of the profile and the profile element width are used as the typical values of β and γ herein, respectively. The effects of surface roughness on the ultrasonic transmission across solid/rubber interfaces have been reported by Drinkwater *et al.* [19]. They suggested that the signal loss spent on solid/rubber interfaces is decreased with decreasing β if γ is constant, and the signal loss decreased with increasing γ if β is constant. The dry-contact ultrasonic device shown in Fig. 1 was used for the transmission. The pressure p is approximately 0.1 MPa because atmospheric pressure and the ultimate pressure of a vacuum pump are 0.101 and 0.007 MPa, respectively. The 100 MHz transducer, of which z_0 is 12.7 mm and $2a$ is 6.35 mm, was used in addition to the former two transducers.

The amplitude spectra of the back-wall echoes, $\eta^{\text{reflection}}(f)$, received by DCUTs using PVC film and SIR sheet and the immersion technique are shown in Fig. 4. These spectra were acquired at the same receiver gain for every transducer, and the values of peak frequency, f_p , of the 30, 50, and 100 MHz transducers in the case of immersion technique are 24.4, 31.7, and 36.6 MHz, respectively. Fig. 4 shows that $\eta^{\text{reflection}}(f)$ of DCUT using PVC film is much larger than that of the immersion technique for all transducers. This is due to the difference in the reflection interface. It is resin/air interface in the case of DCUT, and resin/water interface is formed in the case of immersion technique. However, $\eta^{\text{reflection}}(f)$ of DCUT using SIR sheet is far smaller than any others except the 30 MHz transducer.

The SNR, which is defined by the following equation [20], was determined from the back-wall echoes:

$$\text{SNR} = 10 \cdot \log \frac{S}{N}. \quad (9)$$

Both of S and N are given by:

$$S = \frac{1}{Y} \sum_{y=0}^{Y-1} [E_S(y)]^2, \quad (10)$$

and

$$N = \frac{1}{Y} \sum_{y=0}^{Y-1} [E_N(y)]^2, \quad (11)$$

where E_S and E_N are the echo signal and the noise signal of the length Y , respectively. The signal E_N was acquired from a nonsignal interval recorded with E_S . The SNR of the back-wall echoes for the tried techniques is summarized in Table II. For all used transducers, DCUTs using the films accomplish the higher SNR than that of the immersion technique, but the SNR of DCUT using SIR sheet is the lowest in the tried techniques.

B. Lateral Resolution

The resolution d^{PE} achieved at the focal plane by DCUTs and immersion technique is estimated. The resolution d^{PE} is defined as the separation distance between two sound sources, which can be distinguished clearly with each other, and is estimated from the beam intensity at the focal plane. Generally, the beam intensity is given by the point-spread function (PSF), and it is calculated on the single frequency. However, because the changes in the frequency components occur in the cases of the used broadband transducers, the beam intensity was calculated by adding PSF for each frequency component complexly [21], [22]. Namely, the effective PSF, $\xi_e(r)$, is expressed as follows:

$$\xi_e(r) = \sum_{f_L}^{f_U} \left\{ \left[\frac{2J_1(k_w r a / z_0)}{k_w r a / z_0} \right]^2 \cdot \eta^{\text{reflection}}(f) \right\}, \quad (12)$$

where r is the radial distance from the center axis of the lens; f_L is the lower frequency limit ($= 2.44$ MHz); f_U is the upper frequency limit ($= 100.10$ MHz); and J_1 is the Bessel function of the first kind and first order. The function $\xi_e(r)$ takes its maximum value at $r = 0$.

The ratio $\xi_e(r)/\xi_e(0)$ of the 50 MHz transducer in the cases of DCUTs using PVC film and SIR sheet and the immersion technique is shown in Fig. 5. The velocity C_w used in (12) was 1500 m/s. Fig. 5 shows that $\xi_e(r)/\xi_e(0)$ of DCUT using PVC film is in good agreement with one of the immersion technique, but one of DCUT using SIR sheet is larger than the others at the outside of the center. The increment of $\xi_e(r)/\xi_e(0)$ at the outside leads degradation of d^{PE} . Based on the former definition, the values of

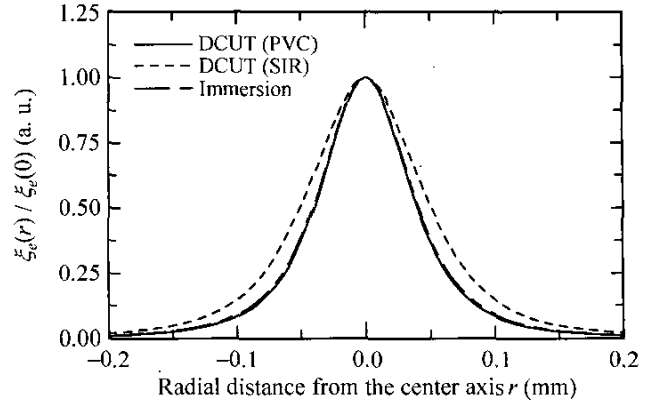


Fig. 5. Effective point-spread function of the 50 MHz transducer in the cases of DCUTs using PVC film and SIR sheet and the immersion technique.

d^{PE} of tried techniques are estimated as shown in Table II. Table II shows that d^{PE} of DCUTs using the films is near to one of the immersion technique for all transducers, and one of DCUT using SIR sheet is the worst in the tried techniques.

C. Contact Coefficient

The coefficient $C^{PE}(f, p, \beta, \gamma)$ at the dry-contact interface formed with the combinations of the inserted films and the acrylic resin is determined by (8). Here, p , β , and γ take constant values as the same resin was tested by different techniques in the air. The properties of the films used in this calculation are given in Table I, and the other data are $Z_s = 3.186 \text{ MNm}^{-3}\text{s}$ and $Z_a = 0.0004 \text{ MNm}^{-3}\text{s}$. The coefficient $\alpha_w(f)$ is given by $25.2 \times 10^{-6} f^2$ 1/mm where f is in megahertz. In addition, the values of $(L_2 - L_1)$ in the cases of the 30, 50, and 100 MHz transducers are 1.2, 1.1, and 0.7 mm, respectively.

The values of $C^{PE}(f_p)$ of the PVC, PE films/resin, and SIR sheet/resin interfaces are summarized in Table II. In the case of SIR sheet/resin interface, the value of $C^{PE}(f_p)$ decreases with increasing the nominal transducer frequency. However, in the case of PE film/resin interface, the values of $C^{PE}(f_p)$ of the 30 and 50 MHz transducers are almost unity, but one of the 100 MHz transducers is fairly small. The decrease of $C^{PE}(f_p)$ is caused by the displacement discontinuity between film or sheet and resin accompanied with ultrasonic transmission. This indicates that the film or sheet comes off from the resin's surface during ultrasonic transmission [16]. The pressure p was approximately 0.1 MPa in this experiment. Because the values of $C^{PE}(f_p)$ change with p , the values of $C^{PE}(f_p)$ in the cases of PE film/resin and SIR sheet/resin interfaces may approach unity if additional p is applied on the interfaces. In contrast with the previous two interfaces, the values of $C^{PE}(f_p)$ of the PVC film/resin interface are almost unity for all transducers. It is suggested that the perfect interface, where the displacement continuity of the film and the resin is maintained, is formed. Also, the efficiency

TABLE II
THE SNR, LATERAL RESOLUTION, AND THE CONTACT COEFFICIENT OF THE DCUT.

Technique	Nominal transducer frequency (MHz)								
	30			50			100		
	SNR (dB)	d^{PE} (μm)	$C^{PE}(f_p)$	SNR (dB)	d^{PE} (μm)	$C^{PE}(f_p)$	SNR (dB)	d^{PE} (μm)	$C^{PE}(f_p)$
DCUT (PVC)	33.7	159	0.91	33.6	65	0.97	30.2	51	0.95
DCUT (PE)	33.7	160	0.93	34.9	66	0.92	25.0	53	0.63
DCUT (SIR)	27.3	177	0.71	17.9	85	0.37	7.0	67	0.21
Immersion	27.6	163	—	25.2	67	—	21.4	49	—

of the dry-contact transmission is not decided by only the acoustical properties of the films such as Z_f and $\alpha_f(f)$. Especially, the SNR and d^{PE} are governed by $C^{PE}(f_p)$ in the case of the 100 MHz transducer.

V. APPLICATION TO ULTRASONIC IMAGING

Two kinds of the IC packages were imaged by the 50 MHz transducer. A PVC film was used for DCUT because it was confirmed to realize the sufficient SNR and high d^{PE} as immersion technique in the previous section. Furthermore, PVC film far excels in durability compared with PE film. For example, the tensile strength of PVC film ranges between 41.3 and 61.9 MPa, and that of the PE film is between 6.9 and 16.5 MPa [23]. The durability is necessary for automated inspection requiring cyclic testing. One of the imaged packages is the dual in-line package (DIP) containing a delamination, and another is a BGA package.

A. Delamination in DIP

The imaged DIP having a size of $18 \times 6 \times 3$ mm contained a delamination between the silicon chip and the chip pad in the epoxy resin. The parameters β and γ of the resin are 0.85 and $141 \mu\text{m}$, respectively, and they are much larger than those of the former acrylic resin. The imaging was performed from the silicon chip side, and the scan pitch was 0.024 mm. Furthermore, DIP was also imaged by DCUT using SIR sheet and the immersion technique for reference.

The acoustic images of the delamination in DIP obtained by DCUTs using PVC film and SIR sheet and the immersion technique are shown in Fig. 6. Fig. 6(a) shows that the delamination part is clearly discriminated from the part without one. Furthermore, the image closely resembles one obtained by the immersion technique in point of the clearness of the image. It is suggested that $C^{PE}(f, p, \beta, \gamma)$ at the PVC film/epoxy resin interface is almost in unity, although the epoxy resin has a rough surface compared with that of the former resin. Although the delamination is also found out in the image obtained by DCUT using SIR sheet, the image is inferior in clearness of the image and the difference of light and shade in the

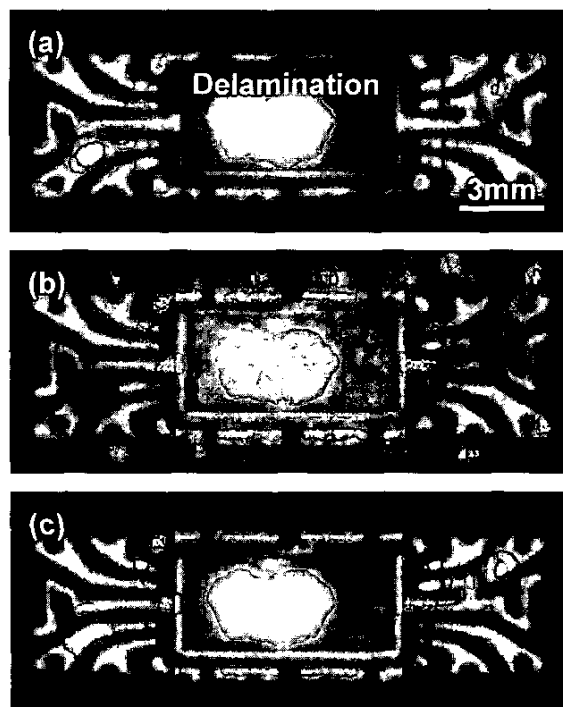


Fig. 6. Acoustic images of the delamination between the silicon chip and the chip pad in DIP. (a) DCUT using PVC film (59 dB). (b) DCUT using SIR sheet (66 dB). (c) Immersion technique (54 dB).

delamination part is larger than the others. This is due to a low SNR in the case of DCUT using the SIR sheet.

B. Solder Joints of BGA

The imaged BGA package having a size of $10.5 \times 8.0 \times 1.1$ mm was already mounted on the printed circuit board (PCB) for a mobile phone by solder joints. The parameters β and γ are 0.06 and $4 \mu\text{m}$, respectively, and they are almost the same as those of the former acrylic resin. The PCB contained some other packages on both sides. The ultrasonic imaging was carried out by pulse-echo mode, and the scan pitch was 0.012 mm. The BGA package also was imaged by the immersion technique for reference.

The acoustic image of the jointing interface between the package substrate and the solder balls obtained by DCUT using PVC film is shown in Fig. 7(a), and the acoustic

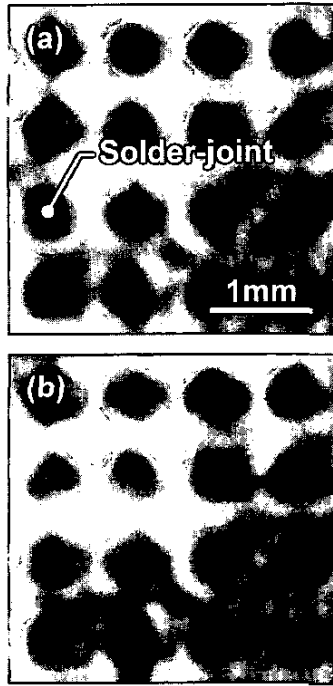


Fig. 7. Acoustic images of the jointing interface between the package substrate and the solder balls (55 dB). (a) DCUT using PVC film. (b) Immersion technique.

image obtained by the immersion technique is shown in Fig. 7(b). Fig. 7(a) shows that the jointing points between the substrate and the solder balls are imaged clearly as one of the immersion technique [Fig. 7(b)]. Especially, it is notable that both images were procured at the same receiver gain.

VI. CONCLUSIONS

The efficiency of the ultrasonic transmission into the dry-contact interface was investigated. The interface was formed by inserting a thin film between water and a sample, and the pressure between the film and the sample was decreased by a vacuum pump. The signal loss accompanied with the dry-contact transmission using various films was determined by the proposed transmission model. When the displacement continuity between the film and the sample is disordered by the transmission of higher frequency ultrasound, the transmission is intercepted at the film/sample interface. The higher frequency ultrasound can be transmitted effectively into the sample by utilizing the optimum film, which can prevent the displacement discontinuity between the film and the sample during ultrasonic transmission. The dry-contact ultrasonic imaging, which had the sufficient SNR and high lateral resolution as immersion technique, was performed on the delamination in a package and the jointing interface of the BGA package without wetting the packages.

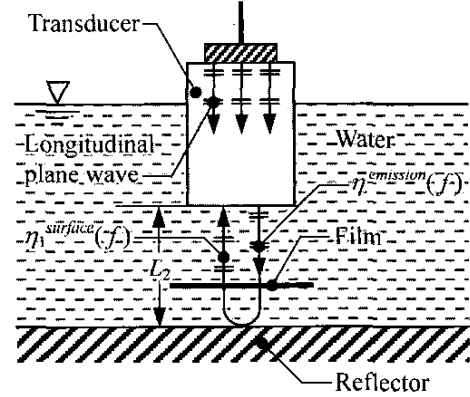


Fig. 8. Experimental setup for determining the attenuation coefficient of a thin film.

APPENDIX A ATTENUATION COEFFICIENT OF THIN FILM

To determine the attenuation coefficient of a thin film, an ultrasonic transmission system shown in Fig. 8 is considered. An emission wave reaches to the reflection wave from the reflector placed in water at normal incidence, and the reflection wave from the reflector's surface is recorded. Here, when a film is inserted between the transducer and the reflector so the film is parallel to the reflector's surface, the reflection wave, $\eta_1^{\text{surface}}(f)$, can be described as:

$$\eta_1^{\text{surface}}(f) = \eta^{\text{emission}}(f) \cdot \alpha_3^{\text{total}}(f) \cdot T_{wfw}(f) \cdot R_{wr} \cdot T_{wfw}(f) \cdot D, \quad (\text{A1})$$

where the subscript r represents the reflector, and

$$\alpha_3^{\text{total}}(f) = \exp \{ - [\alpha_f(f) \cdot 2t_f + \alpha_w(f) \cdot 2L_2] \}. \quad (\text{A2})$$

Furthermore, the reflection wave in the case without the film in the transmission path, $\eta_2^{\text{surface}}(f)$, is given by:

$$\eta_2^{\text{surface}}(f) = \eta^{\text{emission}}(f) \cdot \alpha_4^{\text{total}}(f) \cdot R_{wr} \cdot D, \quad (\text{A3})$$

where

$$\alpha_4^{\text{total}}(f) = \exp \{ - [\alpha_w(f) \cdot 2L_2] \}. \quad (\text{A4})$$

By dividing (A1) by (A3), $\alpha_f(f)$ can be expressed as:

$$\alpha_f(f) = -\frac{1}{2t_f} \ln \left\{ \frac{1}{|T_{wfw}^2(f)|} \cdot Q(f) \right\}. \quad (\text{A5})$$

where $Q(f) = |\eta_1^{\text{surface}}(f) / \eta_2^{\text{surface}}(f)|$.

ACKNOWLEDGMENT

The authors wish to acknowledge Mr. M. Mikami of Tohoku University for his help in the experiment.

REFERENCES

- [1] R. R. Tummalala, in *Fundamentals of Microsystems Packaging*. New York: McGraw-Hill, 2001, pp. 44-79.
- [2] S. Baba, Y. Tomita, M. Matsuo, H. Matsushima, N. Ueda, and O. Nakagawa, "Molded chip scale package for high pin count," *IEEE Trans. Comp., Packag., Manufact. Technol. B*, vol. 21, no. 1, pp. 28-34, 1998.
- [3] C. Neubauer, "Intelligent X-ray inspection for quality control of solder joints," *IEEE Trans. Comp., Packag., Manufact. Technol. C*, vol. 20, no. 2, pp. 111-120, 1997.
- [4] V. Sankaran, A. R. Kalukin, and R. P. Kraft, "Improvements to X-ray laminography for automated inspection of solder joints," *IEEE Trans. Comp., Packag., Manufact. Technol. C*, vol. 21, no. 2, pp. 148-154, 1998.
- [5] K. Yamanaka, Y. Nagata, S. Nakano, T. Koda, H. Nishino, Y. Tsukahara, H. Cho, M. Inada, and A. Satoh, "SAW velocity measurement of crystals and thin films by the phase velocity scanning of interference fringes," *IEEE Trans. Ultrason., Ferroelect., Freq. Contr.*, vol. 42, no. 3, pp. 381-386, 1995.
- [6] Y. Ju, M. Saka, and H. Abé, "NDI of delamination in IC packages using millimeter-waves," *IEEE Trans. Instrum. Meas.*, vol. 50, no. 4, pp. 1019-1024, 2001.
- [7] P. K. Liaw, D. K. Hsu, N. Yu, N. Miriyala, V. Saini, and H. Jeong, "Investigation of metal and ceramic-matrix composites moduli: Experiment and theory," *Acta Mater.*, vol. 44, no. 5, pp. 2101-2113, 1996.
- [8] K.-H. Im, D. K. Hsu, and H. Jeong, "Material property variations and defects of carbon/carbon brake disks monitored by ultrasonic methods," *Composites Part B*, vol. 31, no. 8, pp. 707-713, 2000.
- [9] W. Manthey, N. Kroemer, and V. Mágori, "Ultrasonic transducers and transducer arrays for applications in air," *Meas. Sci. Technol.*, vol. 3, no. 3, pp. 249-261, 1992.
- [10] R. Hickling and S. P. Marin, "The use of ultrasonics for gauging and proximity sensing in air," *J. Acoust. Soc. Amer.*, vol. 79, no. 4, pp. 1151-1160, 1986.
- [11] S. K. Yang, V. V. Varadan, and V. K. Varadan, "Noncontact thickness measurement of wet/dry paint coating using an air-coupled transducer," *Mater. Eval.*, vol. 48, no. 4, pp. 471-474, 1990.
- [12] A. J. Rogovsky, "Development and application of ultrasonic dry-contact and air-contact C-scan systems for nondestructive evaluation of aerospace composites," *Mater. Eval.*, vol. 49, no. 12, pp. 1491-1497, 1991.
- [13] D. W. Schindel, D. A. Hutchins, L. Zou, and M. Sayer, "The design and characterization of micromachined air-coupled capacitance transducers," *IEEE Trans. Ultrason., Ferroelect., Freq. Contr.*, vol. 42, no. 1, pp. 42-50, 1995.
- [14] W. Wright, D. Hutchins, D. Jansen, and D. Schindel, "Air-coupled Lamb wave tomography," *IEEE Trans. Ultrason., Ferroelect., Freq. Contr.*, vol. 44, no. 1, pp. 53-59, 1997.
- [15] H. Tohmyoh and M. Saka, "Development of a dry-contact ultrasonic technique and its application to NDE of IC packages," in *Recent Advances in Experimental Mechanics*. Dordrecht, The Netherlands: Kluwer, 2002, pp. 443-454.
- [16] H. Tohmyoh and M. Saka, "A dry-contact method for transmitting higher frequency components of ultrasound," *Int. J. Appl. Electromag. Mech.*, to be published.
- [17] D. J. Roth, J. D. Kiser, S. M. Swickard, S. A. Szatmary, and D. P. Kerwin, "Quantitative mapping of pore fraction variations in silicon nitride using an ultrasonic contact scan technique," *Res. Nondestr. Eval.*, vol. 6, no. 3, pp. 125-168, 1995.
- [18] A. Kumar, B. Kumar, and Y. Kumar, "A novel method to determine the acoustic impedance of membrane material," *Ultrasonics*, vol. 35, no. 1, pp. 53-56, 1997.
- [19] B. Drinkwater, R. Dwyer-Joyce, and P. Cawley, "A study of the transmission of ultrasound across solid-rubber interfaces," *J. Acoust. Soc. Amer.*, vol. 101, no. 2, pp. 970-981, 1997.
- [20] C. A. Vergers, "Noise in electronic devices," in *Handbook of Electrical Noise: Measurement and Technology*, 2nd ed. Blue Ridge Summit, PA: Tab Professional and Reference Books, 1987, pp. 96-124.
- [21] L. Bechou, Y. Ousten, B. Tregon, F. Marc, Y. Danto, R. Even, and P. Kertesz, "Ultrasonic images interpretation improvement for microassembling technologies characterization," *Microelectron. Reliab.*, vol. 37, no. 10/11, pp. 1787-1790, 1997.
- [22] S. Canumalla, "Resolution of broadband transducers in acoustic microscopy of encapsulated ICs: Transducer selection," *IEEE Trans. Comp. Packag. Technol.*, vol. 22, no. 4, pp. 582-592, 1999.
- [23] C. A. Harper, "Fundamentals of plastics and elastomers," in *Handbook of Plastics and Elastomers*. New York: McGraw-Hill, 1975, pp. 2-121.



Hironori Tohmyoh received the B.Eng. and M.Eng. degrees in mechanical engineering from the University of Electro-Communications, Tokyo, Japan, in 1998 and 2000, respectively.

He is currently a graduate student in the Department of Mechanical Engineering at Tohoku University, Sendai, Japan. His research interest is the application of dry-contact ultrasonic technique to the evaluation of material.



Masumi Saka received the B.Eng. degree in mechanical engineering in 1977 and the Dr.Eng. degree in mechanical engineering in 1982, both from Tohoku University, Sendai, Japan. He became a professor at Tohoku University in 1993.

Dr. Saka received the Japan Society of Mechanical Engineers Medals in 1992 and 2000, the Best Paper Award from the Japanese Society for Non-Destructive Inspection in 1991, the R. E. Peterson Award in 1992 from the Society for Experimental Mechanics, and other awards on sensing and evaluation of materials systems.